



## Methanol sensing properties of honeycomb-like SnO<sub>2</sub> grown on silicon nanoporous pillar array

Ling Li Wang <sup>a,\*</sup>, Zi Jiong Li <sup>a</sup>, Lei Luo <sup>b</sup>, Cheng Zhou Zhao <sup>a</sup>, Li Ping Kang <sup>a</sup>, De Wei Liu <sup>a</sup>

<sup>a</sup> Department of Physics and Electronic Engineering, Zhengzhou University of Light Industry, Zhengzhou 450002, China

<sup>b</sup> Nuclear and Radiation Safety Monitoring Center in Shandong Province, Jinan 250013, China

### ARTICLE INFO

#### Article history:

Received 28 February 2016

Received in revised form

23 April 2016

Accepted 25 April 2016

Available online 27 April 2016

#### Keywords:

Tin oxide (SnO<sub>2</sub>)

Silicon nanoporous pillar array (Si-NPA)

Methanol sensor

### ABSTRACT

A honeycomb-like tin oxide (SnO<sub>2</sub>) film was grown on the silicon nanoporous pillar array (Si-NPA) substrate by a chemical vapor deposition (CVD) method. After SnO<sub>2</sub> growth the pillar morphological characteristic of Si-NPA was inherited and the honeycomb-like SnO<sub>2</sub> film surface was porous and crumpled, with the average nanopores sizes of ~50 nm. A methanol sensor was made based on SnO<sub>2</sub>/Si-NPA and its methanol sensing properties were characterized. It was found that the optimum working temperature of the sensor was determined to be 320 °C. The device response increased from ~3.6 to 38.9 monotonously with the methanol concentration changed from 10 to 500 ppm. The response and recovery times were measured to be ~4–13 and ~9–11 s, respectively. Furthermore, the sensor was proved to be excellent selective to methanol. Our results indicate that SnO<sub>2</sub>/Si-NPA might be a candidate material for fabricating practical methanol sensors.

© 2016 Elsevier B.V. All rights reserved.

## 1. Introduction

Gas sensors have been used in a wide variety of applications, such as environment monitoring, industrial process control, and agricultural or medical detection and analysis [1–5]. In recent years, the attention to pollution free environment has increased day by day, due to the rising emission of toxic and harmful gases in the atmosphere. As a common chemical material, methanol has been widely used in many industry productions such as antifreezes, fuels, colors, and drugs. However, methanol has very strong toxicity to human's blood and nervous system, hence it is essential to develop reliable and selective sensors detecting methanol in ambient air [6,7]. In the past decade, there has been increasing interest in developing high performance gas sensors based on metal oxide semiconductor nanostructures, such as ZnO [8–10], SnO<sub>2</sub> [11,12], In<sub>2</sub>O<sub>3</sub> [13,14] and TiO<sub>2</sub> [15,16]. As n-type wide band gap semiconductor, SnO<sub>2</sub> has been demonstrated as a potential candidate for gas sensors [17–20].

Material structure plays an important role in gas sensing properties. Recently, numbers of nanostructures have been extensively utilized in gas sensors due to their large specific surface area

and relatively high sensitivity [21–24]. Especially lots of researches have devoted to improve the device performances of gas sensors based on various SnO<sub>2</sub> nanostructures such as nanowires [25–27], nanotubes [28,29], hollow spheres [30–32], and flowerlike nanostructures [33] in the past several years. In the previous studies, we reported the preparation and characterization of silicon nanoporous pillar array (Si-NPA), a unique silicon hierarchical structure prepared by a hydrothermal etching method [34]. It has been illustrated that Si-NPA is an ideal template for materials growth and the composite materials show excellent sensing properties [35–37], such as SiC/Si-NPA which exhibited high sensitivity, repeatability and long-term stability to H<sub>2</sub>S [38].

In this paper, a honeycomb-like SnO<sub>2</sub> film was grown on Si-NPA substrate by a chemical vapor deposition (CVD) method. The methanol sensing properties of SnO<sub>2</sub>/Si-NPA, including the optimum working temperature, response, response and recovery times, and selectivity were studied systematically. Our results indicated that SnO<sub>2</sub>/Si-NPA might be an ideal sensing material for fabricating practical methanol sensors.

## 2. Experimental details

As described in detail elsewhere [34], the Si-NPA substrate was prepared by hydrothermally etching (111) oriented, heavily boron-doped single crystal silicon (sc-Si) wafers (rectangles specified by

\* Corresponding author.

E-mail address: [2013064@zzuli.edu.cn](mailto:2013064@zzuli.edu.cn) (L.L. Wang).

15 mm × 15 mm) in the solution of hydrofluoric acid (HF) containing ferric nitrate ( $\text{Fe}(\text{NO}_3)_3$ ). The honeycomb-like  $\text{SnO}_2$  was grown on Si-NPA through the chemical-vapor-deposition (CVD) method in a horizontal tube furnace (Fig. 1(a)). High-purity tin powder was used as Sn source, while Si-NPA as the substrate was placed 10 cm away from the Sn source downstream to the carrier gas. After the chamber inner pressure was pumped down to ~10 Pa, high-purity argon with a rate of 200 standard cubic centimeters per minute (sccm) and oxygen with rates of 50 sccm flows were introduced, respectively. Then tube chamber was heated up to 900 °C with a rate of 10 °C/min and then remains constant for 30 min. Finally, the furnace was cooled down to room temperature with a rate of 10 °C/min. The chamber inner pressure was maintained at 450 Pa during the whole CVD process and a schematic diagram of the preparation process of  $\text{SnO}_2$ /Si-NPA was shown in Fig. 1(b).

The sensor was prepared through magnetron sputtering coplanar interdigital silver electrodes onto  $\text{SnO}_2$ /Si-NPA sample. The schematic diagram of the sensor was illustrated in Fig. 2(a). The gas sensing properties of the sensor were measured on CGS-1TP gas sensing measurement system (Beijing Elite Tech Co., Ltd, China). The analysis system offered an external temperature control (from room temperature to 500 °C with a precision of 1 °C), which could conductively adjust the sensor temperature directly. Two probes were pressed on sensor substrates to export electrical signals. When the resistances of the sensors were stable, saturated target gas was injected into the test chamber (18 L in volume) by a micro-injector through a rubber plug. The saturated target gas was mixed with air by two fans in the analysis system. After the sensor resistances reached new constant values, the test chamber was opened to recover the sensors in air. The sensor resistance and sensitivity were collected and analyzed by the system in real time. A photograph of the gas sensing analysis system was shown in Fig. 2(b). The crystal structure and surface morphology of as-prepared  $\text{SnO}_2$ /Si-NPA were characterized by an X-ray diffractometer (XRD, Panalytical X' Pert Pro) and a field-emission scanning electron microscope (FE-SEM, JSM 6700F), respectively. All the measurements were carried out at room temperature under atmospheric pressure.

### 3. Results and discussion

#### 3.1. Crystal structure and surface morphology

Fig. 3 shows the XRD pattern of as-prepared  $\text{SnO}_2$ /Si-NPA. Here nine diffraction peaks were observed and all of them were indexed to tetragonal rutile  $\text{SnO}_2$ , which indicates the growth of  $\text{SnO}_2$  on Si-

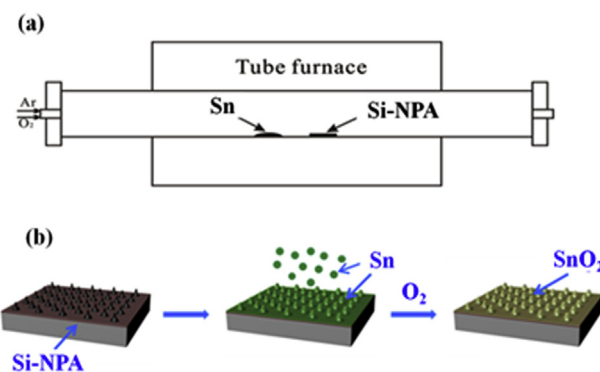


Fig. 1. A schematic diagram of tube furnace (a), and preparation process of  $\text{SnO}_2$ /Si-NPA (b).

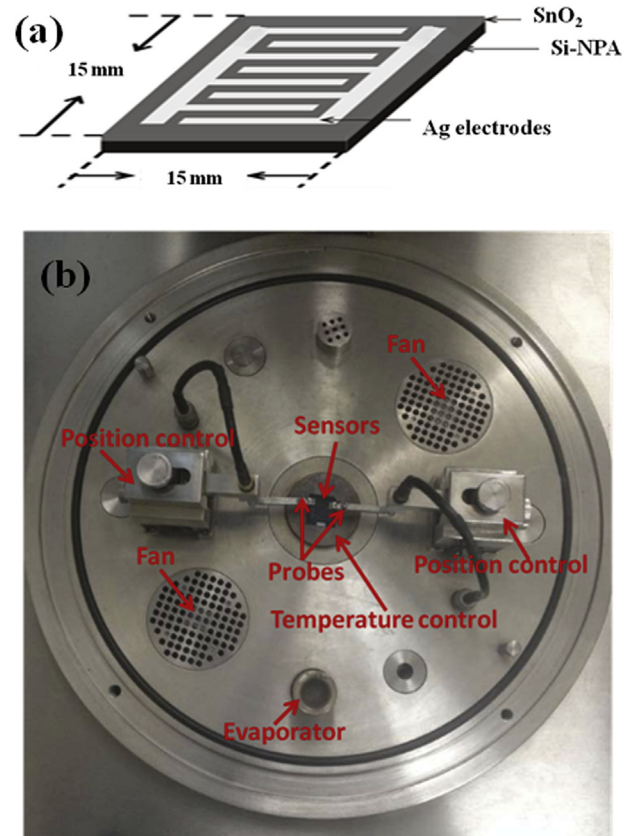


Fig. 2. (a) A schematic diagram to illustrate the structure of  $\text{SnO}_2$ /Si-NPA methanol sensor. (b) A photograph of the gas sensing analysis system.

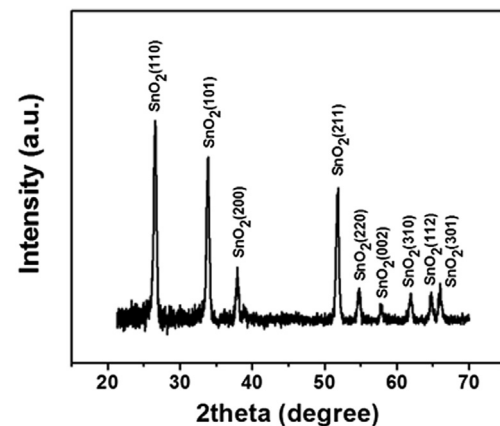
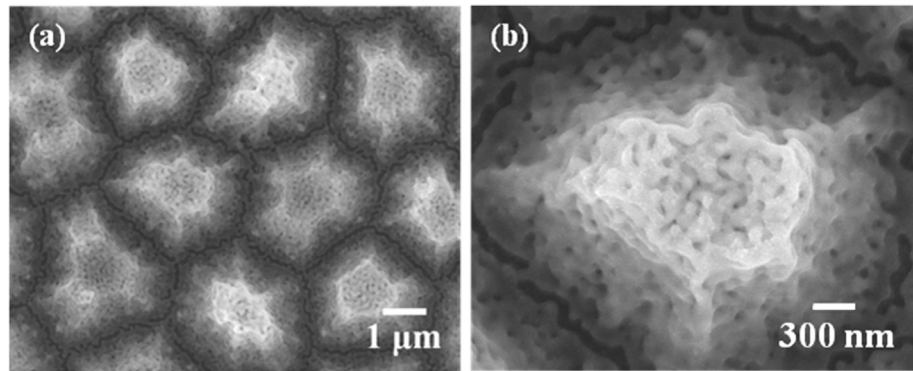


Fig. 3. The XRD pattern of  $\text{SnO}_2$ /Si-NPA.

NPA. As has been characterized previously [34], Si-NPA is a Si hierarchical structure characterized by a large area and regular array composed of micron-sized, quasi-identical and highly-porous Si pillars. After the CVD process, the surface morphology of  $\text{SnO}_2$ /Si-NPA was presented in Fig. 4. Observed from the low magnification FE-SEM image (Fig. 4(a)), honeycomb-like  $\text{SnO}_2$  film was grown on Si-NPA, with the pillars of Si-NPA still well-separated and the morphological characteristic of the pillar array of Si-NPA is inherited. From the FE-SEM image with a larger magnification (Fig. 4(b)), the honeycomb-like  $\text{SnO}_2$  film surface was porous and crumpled, with an average nanopores size of ~50 nm. Obviously,



**Fig. 4.** The FE-SEM images of  $\text{SnO}_2/\text{Si-NPA}$ .

the regular array as well as the hierarchical features of honeycomb-like  $\text{SnO}_2/\text{Si-NPA}$  could provide an effective path for gas transport and an enlarged specific area for gas sensing, and both of them might enhance the sensing effects.

### 3.2. Methanol-sensing properties

#### 3.2.1. Response and optimum operating temperature

It is well known that the sensing properties of a resistive-type metal oxide semiconductor gas sensor highly depend upon its working temperature. In order to determine the optimum operating temperature of  $\text{SnO}_2/\text{Si-NPA}$ , the responses of the sensor to methanol with concentrations of 50, 100 and 200 ppm, were measured as a function of temperature (200, 240, 280, 320, 360 and 400 °C, respectively). Fig. 5 shows the corresponding response-temperature curves, where the response was defined as  $R = R_a/R_g$ , where  $R_a$  represented the measuring resistance of the sensor in ambient air and  $R_g$  the resistance of the sensor in the target gas. Obviously, the response-temperature curves measured with different methanol concentrations show a similar evolution trend. When the operating temperature increases from 200 to 300 °C, all the responses of the sensor show an initial slow increase, and then the responses increase much more rapidly between 300 and 320 °C. However, the responses all decreases when the operating temperature higher than 320 °C in the testing range. Obviously, the maximum response was obtained at 320 °C for all the three curves. Therefore it could be concluded that the optimum work temperature of  $\text{SnO}_2/\text{Si-NPA}$  is 320 °C, and all the following measurements would be carried out at this temperature.

Fig. 6 shows the response of  $\text{SnO}_2/\text{Si-NPA}$  sensor exposed to methanol with concentrations of 10, 25, 50, 100, 200, 300, 400 and

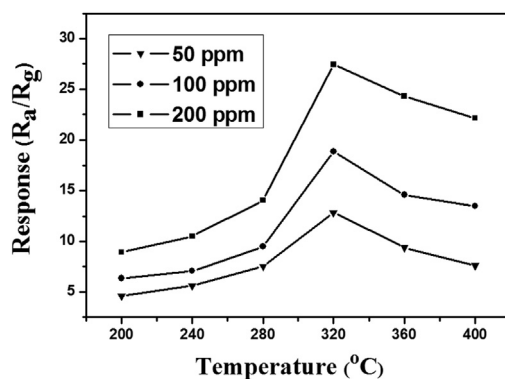


**Fig. 5.** The response-temperature curves of  $\text{SnO}_2/\text{Si-NPA}$  sensor.

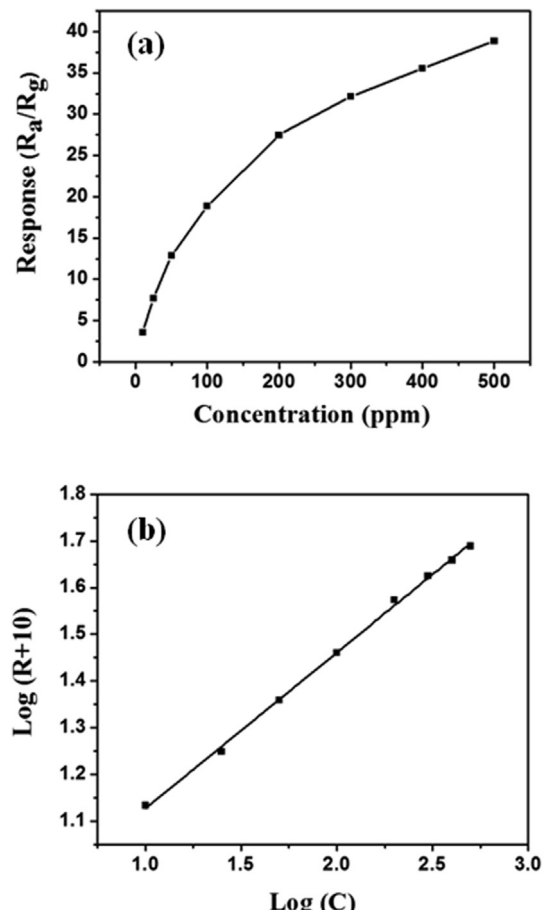


**Fig. 6.** (a) The response-concentration curve of  $\text{SnO}_2/\text{Si-NPA}$  sensor operated at 320 °C. (b) the corresponding  $\log(R + 10)$  versus  $\log(C)$  curve transformed from the data presented in (a).

500 ppm at 320 °C, respectively. When the methanol concentration changed from 10 to 500 ppm, the device response increased from ~3.6 to 38.9 monotonously, indicating that  $\text{SnO}_2/\text{Si-NPA}$  might be a suitable material for methanol detection. To obtain a linear response curve for practical usage, suitable mathematical data transformation was the most commonly used method. Fig. 6(b) represents a chart of logarithm of the response of the sensor ( $R + 10$ ) versus the logarithm of methanol concentration ( $C$ ) transformed from the data of Fig. 6(a). The line is the corresponding linear fitting results, with the adjusted  $R^2$  value of 0.9985.

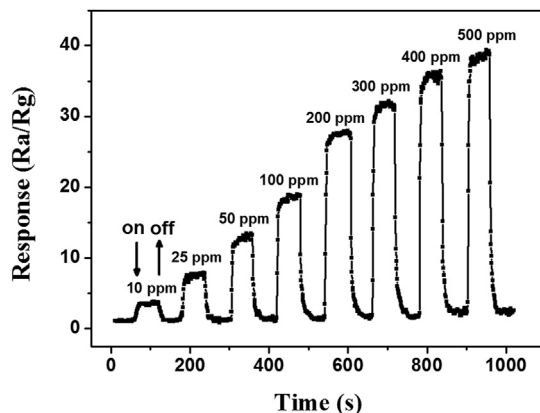
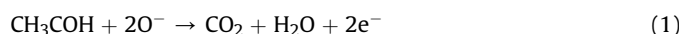


**Fig. 7.** The transient response-recovery of  $\text{SnO}_2/\text{Si-NPA}$  sensor to methanol at different gas concentrations at  $320\text{ }^\circ\text{C}$ .

The results suggest that the response of the sensor based on  $\text{SnO}_2/\text{Si-NPA}$  has a good linear relationship with the methanol concentration in the range of 10–500 ppm in logarithmic form.

The high response of the sensor should be attributed to the intrinsic physical and chemical properties of as-prepared honeycomb-like  $\text{SnO}_2/\text{Si-NPA}$ . According to the surface charge model proposed for explaining the sensing mechanism of oxide semiconductors [39–41], the change of resistance is due to the species and amount of chemisorbed oxygen on the surface. In the case of honeycomb-like  $\text{SnO}_2/\text{Si-NPA}$ , when the sensor was exposed to air the resistance is determined by the concentration of absorbed oxygen ions ( $\text{O}^-$ ,  $\text{O}_2^-$  and  $\text{O}_2$ ) which trap electrons leading to the resistance increasing. When the sensor was exposed to the methanol, the methanol molecule would react with the adsorbed oxygen species reducing their concentration and the sensor resistance would decrease. The corresponding reactions on the sensor surface would be following [42,43].



When the sensor is exposed to the air, the  $\text{SnO}_2/\text{Si-NPA}$  sensor recovers to the original electronic state again. In addition, both the pillar structure and the enlarged specific surface area of the honeycomb-like  $\text{SnO}_2/\text{Si-NPA}$  with porous crumpled surface contribute greatly to the high response. For porous sensing materials, the target gas molecules may diffuse into both the surface and the inner layers of the sensing film and interact with the surface oxygen adsorbed on the interior grains. There are plenty of pores which provide more active sites, so they may adsorb more gas molecules and consequently the sensitivity will increase [44–47]. The results indicated that  $\text{SnO}_2/\text{Si-NPA}$  has both the high sensitivity and the linearity of the logarithmic response-concentration, and would be a potential sensing material for methanol detection.

### 3.2.2. Response/recovery times and measurement reproducibility

Quick response and recovery properties are vital for gas sensors practical applications. Fig. 7 represents the transient response curve of the  $\text{SnO}_2/\text{Si-NPA}$  sensor to methanol gas with different concentrations of 10, 25, 50, 100, 200, 300, 400, and 500 ppm at  $320\text{ }^\circ\text{C}$ . It can be seen that the response of the sensor increased rapidly after the injection of methanol, and then decreased abruptly to its initial value after the test gas was released. With the response time was defined as the time required for the response variation to reach 90% of the equilibrium value after injecting the test gas into testing chamber, and the recovery time as the time needed for the sensor to return to 10% above the initial response in air after releasing the test gas, the response and recovery times for  $\text{SnO}_2/\text{Si-NPA}$  sensor were calculated to be ~4–13 and ~9–11 s for different methanol concentrations, respectively. Compared with the response and recovery times measured for the methanol gas sensors based on other nanomaterials (Table 1), the relative quick response and recovery times of  $\text{SnO}_2/\text{Si-NPA}$  might be attributed to the unique structural and morphological characteristic of honeycomb-like  $\text{SnO}_2/\text{Si-NPA}$ . The valleys surrounded the pillars constitute a well-connected channel network, which provided an effective pathway for gas transportation and was helpful for the rapid adsorption/desorption of methanol molecules. Furthermore, from the experimental data shown in Fig. 7, it should be noted that  $\text{SnO}_2/\text{Si-NPA}$  sensor possessed good measurement stability and reproducibility among the reversible cycles for different ethanol concentration.

### 3.2.3. Selectivity

The selectivity is also important for gas sensor to practical application [51]. The selectivity of honeycomb-like  $\text{SnO}_2/\text{Si-NPA}$  sensor was investigated by comparing its relative response to methanol with those to methanol, ethanol, acetone, toluene and benzene with the same concentration of 100 ppm for all the four target gases. Fig. 8 shows the relative response of the four target gases, where the relative response is defined as the ratio of the responses of methanol, ethanol, acetone, toluene and benzene to that of methanol. It was found that the responses of methanol, ethanol, acetone, toluene and benzene were only ~14.1%, 36.3%, ~22.7%, ~7.5%, and ~5.9% to that of methanol, respectively. This indicates that as-prepared honeycomb-like  $\text{SnO}_2/\text{Si-NPA}$  sensor exhibits excellent selectivity to methanol at  $320\text{ }^\circ\text{C}$ .

## 4. Conclusions

In conclusion, a honeycomb-like  $\text{SnO}_2$  film was grown on the Si-NPA substrate through CVD method and its methanol sensing properties were characterized. The results showed that  $\text{SnO}_2/\text{Si-NPA}$  inherited the pillar morphological characteristic of Si-NPA, and a methanol sensor with coplanar interdigital electrode arrangements was made based on the sample. The optimum working temperature of the sensor for methanol was determined to be  $320\text{ }^\circ\text{C}$ . The device response increased from ~3.6 to 38.9

**Table 1**

Comparison of the methanol sensing performances of various metal oxide nanostructures.

Sensing materials	Working temperature ( $^\circ\text{C}$ )	Methanol concentration (ppm)	Response ( $R_a/R_g$ )	Response/recovery times (s)	Ref.
$\text{SnO}_2/\text{Si-NPA}$	320	50	7.7	10/9	Present work
		200	27.4	5/10	
$\text{La}_{0.8}\text{Pb}_{0.2}\text{FeO}_3$ nanoparticles	230	200	50	40/75	[48]
Ce-doped $\text{In}_2\text{O}_3$ nanospheres	320	100	35.2	14/10	[39]
$\alpha\text{-Fe}_2\text{O}_3$ hollow spheres	280	10	25.1	8/9	[49]
CdS-doped $\text{SnO}_2$ films	200	5000	70	40/110	[50]

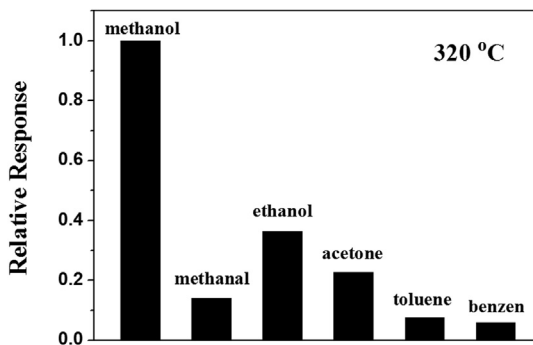


**Fig. 8.** The relative responses of  $\text{SnO}_2/\text{Si-NPA}$  sensor to methanol, methanal, acetone, toluene and benzene measured with the same concentration of 100 ppm at 320 °C.

monotonously when the methanol concentration changed from 10 to 500 ppm, and there was a good linear relationship in logarithmic form between the response and the methanol concentration in the testing range. The response and recovery times were measured to be ~4–13 and ~9–11 s, respectively, and the sensor also exhibited good sensing selectivity. The excellent sensing performance might be attributed to the unique structural and morphological characteristic of honeycomb-like  $\text{SnO}_2/\text{Si-NPA}$ . These results demonstrate that honeycomb-like  $\text{SnO}_2/\text{Si-NPA}$  might be a promising material for fabricating practical methanol gas sensors.

## Acknowledgements

This research was supported by the National Natural Science Foundation of China (No. 11405148), the Frontier Technology Research and Development Program of Zhengzhou (No.141P-QYJS552), the Science and Technology Research Projects of Education Department of Henan Province (No.14B140017).

## References

- [1] Y.H. He, Y.M. Li, Y.X. Chen, Phosphorylation regulates proteolytic efficiency of TEV protease detected by a 5(6)-carboxyfluorescein-pyrene based fluorescent sensor, *Talanta* 150 (2016) 340–345.
- [2] L. Dai, H. Zhou, G. Yang, Y. Li, J. Zhu, L. Wang, Ammonia sensing characteristics of  $\text{La}_{10}\text{Si}_5\text{MgO}_{26}$ -based amperometric-type sensor attached with nano-structured  $\text{CoWO}_4$  sensing electrode, *J. Alloys Compd.* 663 (2016) 86–93.
- [3] W. Yuan, G. Shi, Graphene-based gas sensors, *J. Mater. Chem. A* 1 (2013) 10078–10091.
- [4] Q. He, Z. Zeng, Z. Yin, H. Li, S. Wu, X. Huang, H. Zhang, Fabrication of flexible  $\text{MoS}_2$  thin-film transistor arrays for practical gas-sensing applications, *Small* 8 (2012) 2994–2999.
- [5] L.F. da Silva, V.R. Mastelaro, A.C. Catto, C.A. Escanhoela Jr., S. Bernardini, S.C. Zilio, E. Longo, K. Aguir, Ozone and nitrogen dioxide gas sensor based on a nanostructured  $\text{SrTi}_{0.85}\text{Fe}_{0.15}\text{O}_3$  thin film, *J. Alloys Compd.* 638 (2015) 374–379.
- [6] Y. Li, Y. Chen, H. Xian, Y. Zhou, L. Wang, Cysteamine monolayer inducing the formation of platinum nanoclusters for methanol electrocatalytic oxidation, *Microchim. Acta* 169 (2010) 93–97.
- [7] J.B. Raoof, R. Ojani, S.R. Hosseini, Electrochemical synthesis of a novel platinum nanostructure on a glassy carbon electrode, and its application to the electrooxidation of methanol, *Microchim. Acta* 180 (2013) 879–886.
- [8] M. Zhao, X. Wang, L. Ning, H. He, J. Jia, L. Zhang, X. Li, Synthesis and optical properties of Mg-doped ZnO nanofibers prepared by electrospinning, *J. Alloys Compd.* 507 (2010) 97–100.
- [9] M. Hjiri, R. Dhahri, L. El Mir, A. Bonavita, N. Donato, S.G. Leonardi, G. Neri, CO sensing properties of Ga-doped ZnO prepared by sol–gel route, *J. Alloys Compd.* 634 (2015) 187–192.
- [10] V. Galstyan, E. Comini, C. Baratto, G. Faglia, G. Sberveglieri, Nanostructured ZnO chemical gas sensors, *Ceram. Int.* 41 (2015) 14239–14244.
- [11] S. Xu, J. Gao, L. Wang, K. Kan, Y. Xie, P. Shen, L. Li, K. Shi, Role of the heterojunctions in  $\text{In}_2\text{O}_3$ -composite  $\text{SnO}_2$  nanorod sensors and their remarkable gas-sensing performance for NOx at room temperature, *Nanoscale* 7 (2015) 14643–14651.
- [12] P. Tyagi, A. Sharma, M. Tomar, V. Gupta, Metal oxide catalyst assisted  $\text{SnO}_2$  thin film based SO<sub>2</sub> gas sensor, *Sens. Actuators B* 224 (2016) 282–289.
- [13] J. Zhao, T. Yang, Y. Liu, Z. Wang, X. Li, Y. Sun, Y. Du, Y. Li, G. Lu, Enhancement of  $\text{NO}_2$  gas sensing response based on ordered mesoporous Fe-doped  $\text{In}_2\text{O}_3$ , *Sens. Actuators B* 191 (2014) 806–812.
- [14] S. Elouali, L.G. Bloor, R. Binions, I.P. Parkin, C.J. Carmalt, J.A. Darr, Gas sensing with nano-indium oxides ( $\text{In}_2\text{O}_3$ ) prepared via continuous hydrothermal flow synthesis, *Langmuir* 28 (2012) 1879–1885.
- [15] Z.P. Tshabalala, D.E. Motaung, G.H. Mhlongoa, O.M. Ntwaeborwa, Facile synthesis of improved room temperature gas sensing properties of  $\text{TiO}_2$  nanostructures: effect of acid treatment, *Sens. Actuators B* 224 (2016) 841–856.
- [16] P.M. Perillo, D.F. Rodriguez, Low temperature trimethylamine flexible gas sensor based on  $\text{TiO}_2$  membrane nanotubes, *J. Alloys Compd.* 657 (2016) 765–769.
- [17] B. Wang, L.F. Zhu, Y.H. Yang, N.S. Xu, G.W. Yang, Fabrication of a  $\text{SnO}_2$  nanowire gas sensor and sensor performance for hydrogen, *J. Phys. Chem. C* 112 (2008) 6643–6647.
- [18] Q. Wan, T.H. Wang, Single-crystalline Sb-doped  $\text{SnO}_2$  nanowires: synthesis and gas sensor application, *Chem. Commun.* (2005) 3841–3843.
- [19] A. Kolmakov, D.O. Klenov, Y. Lilach, S. Stemmer, M. Moskovits, Enhanced gas sensing by individual  $\text{SnO}_2$  nanowires and nanobelts functionalized with Pd catalyst particles, *Nano Lett.* 5 (2005) 667–673.
- [20] A. Chowdhuri, V. Gupta, K. Sreenivas, R. Kumar, S. Mozumdar, P.K. Patanjali, Response speed of  $\text{SnO}_2$ -based  $\text{H}_2\text{S}$  gas sensors with CuO nanoparticles, *Appl. Phys. Lett.* 84 (2004) 1180–1182.
- [21] H. Li, F. Meng, J. Liu, Y. Sun, Z. Jin, L. Kong, Y. Hu, J. Liu, Synthesis and gas sensing properties of hierarchical meso-macroporous  $\text{SnO}_2$  for detection of indoor air pollutants, *Sens. Actuators B* 166–167 (2012) 519–525.
- [22] K. Maier, A. Helwig, G. Mueller, P. Hille, M. Eickhoff, Effect of water vapor and surface morphology on the low temperature response of metal oxide semiconductor gas sensors, *Materials* 8 (2015) 6570–6588.
- [23] M. Righetti, A. Amann, S.E. Pratsinis, Breath analysis by nanostructured metal oxides as chemo-resistive gas sensors, *Mater. Today* 18 (2015) 163–171.
- [24] Y.F. Sun, S.B. Liu, F.L. Meng, J.Y. Liu, Z. Jin, L.T. Kong, J.H. Liu, Metal oxide nanostructures and their gas sensing properties: a review, *Sensors* 12 (2012) 2610–2631.
- [25] R. Wang, S. Yang, R. Deng, W. Chen, Y. Liu, H. Zhang, G.S. Zakharova, Enhanced gas sensing properties of  $\text{V}_2\text{O}_5$  nanowires decorated with  $\text{SnO}_2$  nanoparticles to ethanol at room temperature, *RSC Adv.* 5 (2015) 41050–41058.
- [26] H.W. Kim, H.G. Na, Y.J. Kwon, H.Y. Cho, C. Lee, Decoration of Co nanoparticles on ZnO-branched  $\text{SnO}_2$  nanowires to enhance gas sensing, *Sens. Actuators B* 219 (2015) 22–29.
- [27] E.M. El-Maghriby, A. Qurashi, T. Yamazaki, Synthesis of  $\text{SnO}_2$  nanowires their structural and  $\text{H}_2$  gas sensing properties, *Ceram. Int.* 39 (2013) 8475–8480.
- [28] J. Zhang, J. Guo, H. Xu, B. Cao, Reactive-template fabrication of porous  $\text{SnO}_2$  nanotubes and their remarkable gas-sensing performance, *ACS Appl. Mater. Inter.* 5 (2013) 7893–7898.
- [29] Q. Yu, J. Zhu, Z. Xu, X. Huang, Facile synthesis of alpha- $\text{Fe}_2\text{O}_3@\text{SnO}_2$  core-shell heterostructure nanotubes for high performance gas sensors, *Sens. Actuators B* 213 (2015) 27–34.
- [30] X.M. Yin, C.K. Li, M. Zhang, Q.Y. Hao, S. Liu, Q.H. Li, L.B. Chen, T.H. Wang,  $\text{SnO}_2$  monolayer porous hollow spheres as a gas sensor, *Nanotechnology* 20 (2009).
- [31] M. Xu, J. Zhang, S. Wang, X. Guo, H. Xia, Y. Wang, S. Zhang, W. Huang, S. Wu, Gas sensing properties of  $\text{SnO}_2$  hollow spheres/polythiophene inorganic-organic hybrids, *Sens. Actuators B* 146 (2010) 8–13.
- [32] F. Gyger, M. Huebner, C. Feldmann, N. Barsan, U. Weimar, Nanoscale  $\text{SnO}_2$  hollow spheres and their application as a gas-sensing material, *Chem. Mater.* 22 (2010) 4821–4827.
- [33] H. Ren, W. Zhao, L. Wang, S.O. Ryu, C. Gu, Preparation of porous flower-like  $\text{SnO}_2$  micro/nano structures and their enhanced gas sensing property, *J. Alloys Compd.* 653 (2015) 611–618.
- [34] H.J. Xu, X.J. Li, Silicon nanoporous pillar array: a silicon hierarchical structure with high light absorption and triple-band photoluminescence, *Opt. Express* 16 (2008) 2933–2941.
- [35] L.L. Wang, H.Y. Wang, W.C. Wang, K. Li, X.C. Wang, X.J. Li, Capacitive humidity sensing properties of ZnO cauliflower grown on silicon nanoporous pillar array, *Sens. Actuators B* 177 (2013) 740–744.
- [36] H.Y. Wang, Y.Q. Wang, Q.F. Hu, X.J. Li, Capacitive humidity sensing properties of SiC nanowires grown on silicon nanoporous pillar array, *Sens. Actuators B* 166 (2012) 451–456.
- [37] H.Y. Wang, X.J. Li, Capacitive humidity-sensitivity of carbonized silicon nanoporous pillar array, *Mater. Lett.* 64 (2010) 1268–1270.
- [38] H.Y. Wang, Y.Q. Wang, H.Y. Chen, X.J. Li, Room-temperature  $\text{H}_2\text{S}$  gas sensing properties of carbonized silicon nanoporous pillar array, *Thin Solid Films* 520 (2012) 4436–4438.
- [39] N. Barsan, U. Weimar, Conduction model of metal oxide gas sensors, *J. Electroceram.* 7 143–167.
- [40] C. Wang, L. Yin, L. Zhang, D. Xiang, R. Gao, Metal oxide gas sensors: sensitivity and influencing factors, *Sensors* 10 (2010) 2088–2106.
- [41] M. Gardon, J.M. Guilemany, A review on fabrication, sensing mechanisms and performance of metal oxide gas sensors, *J. Mater. Sci. Mater. El.* 24 (2013) 1410–1421.
- [42] P.A. Murade, V.S. Sangawar, G.N. Chaudhari, V.D. Kapse, A.U. Bajpeye, Acetone gas-sensing performance of Sr-doped nanostructured  $\text{LaFeO}_3$  semiconductor prepared by citrate sol–gel route, *Curr. Appl. Phys.* 11 (2011) 451–456.

- [43] D. Han, P. Song, S. Zhang, H. Zhang, Q. Xu, Q. Wang, Enhanced methanol gas-sensing performance of Ce-doped  $\text{In}_2\text{O}_3$  porous nanospheres prepared by hydrothermal method, *Sens. Actuators B* 216 (2015) 488–496.
- [44] F. Meng, N. Hou, Z. Jin, B. Sun, W. Li, X. Xiao, C. Wang, M. Li, J. Liu, Sub-ppb detection of acetone using Au-modified flower-like hierarchical  $\text{ZnO}$  structures, *Sens. Actuators B* 219 (2015) 209–217.
- [45] F. Meng, N. Hou, S. Ge, B. Sun, Z. Jin, W. Shen, L. Kong, Z. Guo, Y. Sun, H. Wu, C. Wang, M. Li, Flower-like hierarchical structures consisting of porous single-crystalline  $\text{ZnO}$  nanosheets and their gas sensing properties to volatile organic compounds (VOCs), *J. Alloys Compd.* 626 (2015) 124–130.
- [46] F. Meng, N. Hou, Z. Jin, B. Sun, Z. Guo, L. Kong, X. Xiao, H. Wu, M. Li, J. Liu, Ag-decorated ultra-thin porous single-crystalline  $\text{ZnO}$  nanosheets prepared by sunlight induced solvent reduction and their highly sensitive detection of ethanol, *Sens. Actuators B* 209 (2015) 975–982.
- [47] H. Li, F. Meng, J. Liu, Y. Sun, Z. Jin, L. Kong, Y. Hu, J. Liu, Synthesis and gas sensing properties of hierarchical meso-macroporous  $\text{SnO}_2$  for detection of indoor air pollutants, *Sens. Actuators B* 166–167 (2012) 519–525.
- [48] C. Doroftei, P.D. Popa, F. Iacomi, Synthesis of nanocrystalline  $\text{La-Pb-Fe-O}$  perovskite and methanol-sensing characteristics, *Sens. Actuators B* 161 (2012) 977–981.
- [49] H.M. Yang, S.Y. Ma, G.J. Yang, W.X. Jin, T.T. Wang, X.H. Jiang, W.Q. Li, High sensitive and low concentration detection of methanol by a gas sensor based on one-step synthesis  $\alpha\text{-Fe}_2\text{O}_3$  hollow spheres, *Mater. Lett.* 169 (2016) 73–76.
- [50] L. Yadava, R. Verma, R. Dwivedi, Sensing properties of  $\text{CdS}$ -doped tin oxide thick film gas sensor, *Sens. Actuators B* 144 (2010) 37–42.
- [51] L.O. Péres, R.W.C. Li, E.Y. Yamauchi, R. Lippi, J. Gruber, Conductive polymer gas sensor for quantitative detection of methanol in Brazilian sugar-cane spirit, *Food Chem.* 130 (2012) 1105–1107.